VLF, magnetic bay, and Pi2 substorm signatures at auroral and midlatitude ground stations

A. J. Smith, M. P. Freeman, and S. Hunter

British Antarctic Survey, Cambridge, UK

D. K. Milling

Department of Physics, University of York, York, UK

[1]   A superposed epoch analysis of $100-300$ substorms is performed to determine the median size and shape of the substorm-associated VLF chorus, magnetic bay, and Pi2 pulsation burst observed at the near-auroral Halley research station, Antarctica, and at the midlatitude Faraday station at three different local times (2230, 2330, 0130 MLT). The spatial and temporal properties of the magnetic bay signatures are compared with the University of York implementation of the Kisabeth–Rostoker substorm current wedge (SCW) model and the Weimer pulse model, respectively. These constitute the best analytical models of the substorm to date. It is shown that the polarities and relative amplitudes of the observed magnetic bays in the H, D, and Z components at Halley at midnight MLT and at Faraday in the premidnight sector are consistent with the York model for a SCW 3 hours wide in MLT with its westward electrojet at $67°$S magnetic latitude. In particular the little-discussed Z component of the bay agrees with the model and is shown to be the clearest substorm signature of the three components, especially at midlatitude. The midnight and postmidnight bays are similar to the premidnight case but progressively smaller and cannot be fully reconciled with the model. The shape of the H and Z bays at Halley and the D bays at Faraday fit a normalized Weimer pulse well, with Weimer's 2 h^{-1} recovery rate, but the other components do not. The D component at Halley and H at Faraday do fit the Weimer pulse shape but with a faster recovery rate of 4 h^{-1}. It is proposed that this is due to the effect of a decaying current in the SCW combining with the geometrical effect of changing SCW configuration and position relative to the observing station. The Z component at Faraday recovers more slowly than the 2 h^{-1} Weimer prediction; we cannot explain this. Secondary bays at Halley and Faraday show a clear tendency to recur after 2 hours. Inflection points just prior to onset at Halley and Faraday are argued to be related to reduced convection associated with northward turning of the IMF. The median substorm signature at Halley in the Pi2 frequency band ($7-25$ mHz) is well correlated with the bay structure, showing that it is part of a broader band, possibly turbulent, spectrum in the substorm-dependent DP2 current. There is evidence of a minor additional narrow band component occurring at substorm onset. This is the dominant signal at Faraday which shows the classic midlatitude substorm signature, a short Pi2 pulsation burst at onset, that decreases progressively in intensity with increasing local time, implying a source region biased to the evening side or else preferred propagation to the east from a near-midnight source.   *INDEX TERMS:* 2788 Magnetospheric Physics: Storms and substorms; 2708 Magnetospheric Physics: Current systems (2409); 2409 Ionosphere: Current systems (2708); 2704 Magnetospheric Physics: Auroral phenomena (2407); *KEYWORDS:* substorm, current wedge, Pi2, chorus, magnetic bay

1.   Introduction

[2]   Substorms vary greatly from event to event and appear differently depending on the observation location and technique. The textbook "typical event" is rarely seen. In a previous paper [*Smith et al.*, 1999] we used a superposed epoch analysis to establish the typical magnetic bay response to the substorm current wedge as observed by magnetometers at a near-auroral-zone ground station (Halley, Antarctica). The rationale was to use a large number of events in order to extract the essential and persistent features

of the substorm response. We used a normalization procedure and took a median rather than a mean of the ensemble of cases, so that large and small (or distant and near) events carried equal weight, in order that the results would not be skewed by a few unusually large events.

[3] To identify the epoch of a substorm expansion phase onset, we used the SCE (substorm chorus event) signature [*Smith et al.*, 1996; *Smith*, 1997], which is sensitive to the whistler mode waves generated by energetic electrons injected at onset. The ground SCE is perhaps a less familiar substorm signature than some others but has the advantage that it is observed independently of the magnetometers, is easy to identify in the data, and usually has a well-defined onset time. A single ground VLF station can detect SCEs originating over a range of L-shells and longitudes. For these reasons we have assembled a large database of event times (over 2500) from SCEs observed at Halley since 1992 when the VELOX VLF/ELF receiver began operating, and here we use subsets of events drawn from that database. A disadvantage of our technique for identifying substorms is that because the injected electrons drift eastward, the SCE is seen only when the observing station is to the east of the injection region, typically from just before local magnetic midnight until dawn.

[4] The main aim of the present study is to apply the *Smith et al.* [1999] approach to investigate the typical substorm-related magnetic bay response at a lower latitude ground station (Faraday/Vernadsky, Antarctica). The results are discussed in terms of the substorm current wedge model. Although there is an extensive literature on this subject, there have been relatively few statistical studies. *Caan et al.* [1978] carried out a superposed epoch analysis of ~1800 substorms to derive the average substorm signatures in midlatitude magnetograms at four local times (00, 06, 12, and 18 hours), in auroral zone magnetograms at two local times (17 hours and 24 hours), and in the AE, AL, and AU indices. The epochs were onset times of the substorms derived from a pattern recognition analysis of midlatitude magnetograms. *Weimer* [1994] did a similar analysis for AE, AL, and AU for 55 events, using AE to determine the onset times. The study by *Kamide and Kroehl* [1994] was for 42 relatively large substorm events in which they determined the average substorm signature in auroral zone H-component ground magnetograms at three local times (00, 06, 18 hours), relative to quiet conditions. The data were not direct observations but were computed from the AL index, and the reference epoch was taken to be the peak of the 00 hour data rather than the substorm onset time.

[5] In this paper we use a superposed epoch analysis to determine the average substorm effect first for the near-auroral Halley station at local midnight (for comparison with *Smith et al.*, [1999]) and then for the midlatitude Faraday station at three local times (premidnight, near-midnight, and postmidnight), more closely spaced than the above-mentioned studies. The numbers of substorms used in the averaging (123, 282, 189, and 136, respectively) were less than *Caan et al.* [1978] but larger than *Weimer* [1994] and *Kamide and Kroehl* [1994]. Like *Caan et al.* [1978] we include the midlatitude Z-component which has otherwise been little treated in past work. We also analyze Pi2 magnetic variations (frequencies 7–25 mHz) at both the

near-auroral and midlatitude stations using the same approach. An important difference between this paper and previous work is that the set of epochs is defined without any reference to the magnetic data, thus avoiding a possible source of bias. The substorm onsets are determined from substorm chorus events which serve as a ground-observed proxy for the injection of energetic electron fluxes into the ring current at the expansion phase onset.

2. Data Sources

[6] In this paper we use ELF/VLF radio wave data from the VELOX instrument at Halley station (76°S, 27°W, L = 4.3) [*Smith*, 1995], magnetic data from the three-component fluxgate magnetometer at Halley [*Dudeney et al.*, 1995], and magnetic data from the similar magnetometer at the Argentine Islands geomagnetic observatory, Faraday station (65°S, 64°W, L = 2.3) [*Cotton and Simmons*, 1986]. Faraday was renamed Vernadsky when it was taken over by the Ukraine in February 1996, but for simplicity it will be referred to throughout this paper as "Faraday" even though we have used data from both before and after the name change. The time resolution of the Halley magnetometer data is 1 s whereas that of the Faraday data is 20 s. The amplitude resolution is 1 nT in both cases. The three magnetic components are H (positive northward in the local magnetic frame), D (positive eastward), and Z (positive upward). Note that our sign convention for Z is the opposite of that normally used in the Northern Hemisphere.

3. Analysis and Results

3.1. A Sample Event

[7] We first present an event which exemplifies the data contributing to the superposed epoch analyses described later. Figure 1 shows the magnetic field and ELF/VLF wave response at Halley and Faraday to a substorm which occurred close to magnetic midnight at Halley (~3 UT), when Faraday was still in the evening sector (~2230 MLT). The characteristics of the SCE (Figure 1b) and magnetic bay (Figure 1d) observed at Halley are typical of events previously published, e.g. in Plate 1 of *Smith et al.* [1999]. The epoch of the SCE, defined as the time at which the signal in the 1.5 kHz channel begins to increase above the preevent level, is marked by the arrow. This time is indicated by the vertical dotted line in the other panels and is seen from Figure 1a to be close to the time at which the AE index began to increase (i.e., the substorm expansion phase onset). The magnetic bay was negative in H, close to zero in D, and negative in Z, as is commonly observed at Halley which is usually located a little equatorward of the auroral oval at midnight.

[8] At Faraday, premidnight and well equatorward of the oval, the magnetic bay (Figure 1c) was positive in H, negative in D, and close to zero in Z. The deviations in all components were much smaller in magnitude than at Halley (note the difference in scales between Figures 1c and 1d). The signs of the changes are consistent with *Rostoker* [1972] for a low-latitude station when translated to the Southern Hemisphere (D and Z change sign but not H), and account is taken of our opposite sign convention for Z. The small oscillations near the substorm onset were mainly
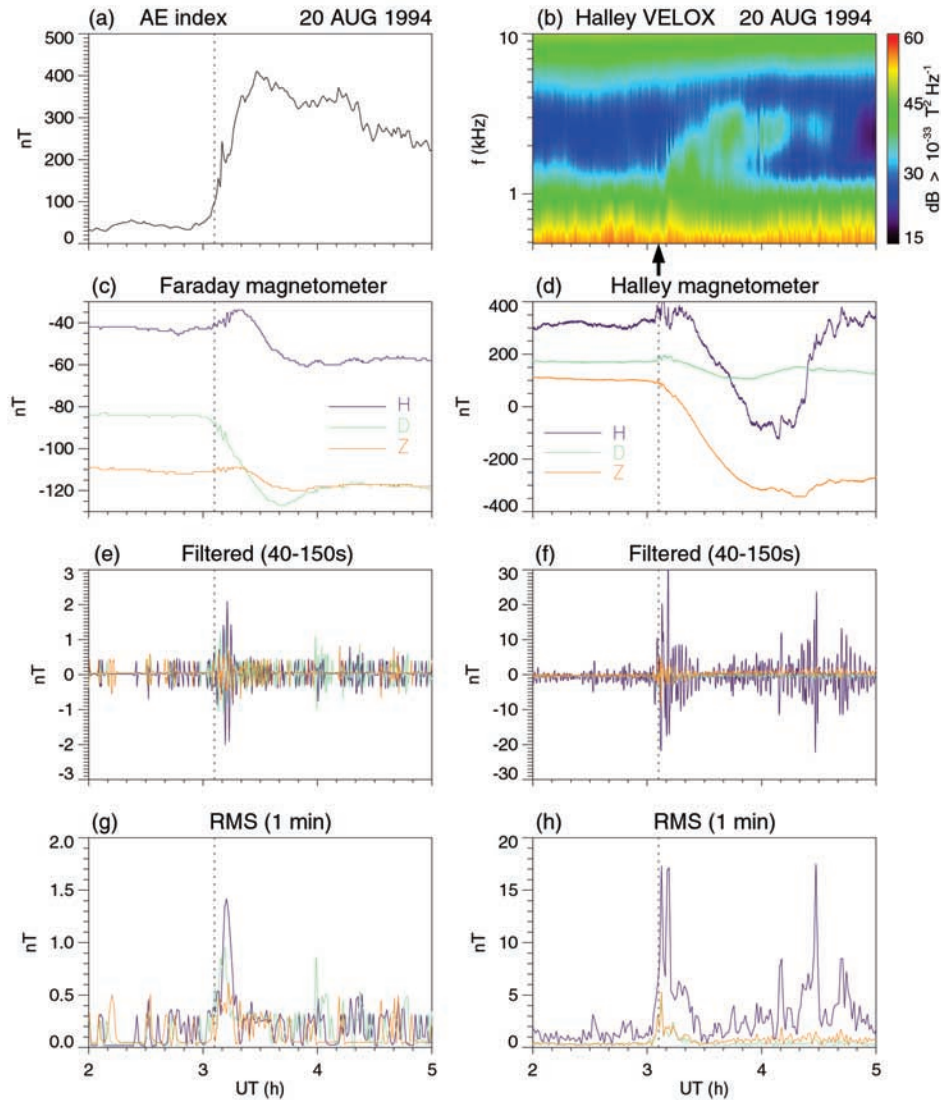
Figure 1. Magnetic field and ELF/VLF wave observations at Halley and Faraday around the time of a substorm which occurred just after 0300 UT on 20 August 1994. (a) The Auroral Electrojet index. (b) A spectrogram from the Halley VELOX VLF/ELF wave receiver, showing the SCE. The intensities in the eight quasi-logarithmically spaced VELOX frequency channels are interpolated onto a log f scale with a 1-min time resolution. The arrow indicates the start of the SCE in the 1.5 kHz channel. This time is shown by the vertical dotted line in the other panels. (c) The three components of magnetic field variation (H, D, Z, i.e., in the north, east, and up directions) measured by the Faraday fluxgate magnetometer. (d) Same as Figure 1c but for the Halley magnetometer. (e) and (f) The signals of Figures 1c and 1d, bandpass-filtered in the range $40-150$ s ($7-25$ mHz). (g) and (h) 1-minute averages of the root mean squares of the signals in Figures 1e and 1f.

in the Pi2 frequency band and have been extracted using a $40-150$ s ($7-25$ mHz) bandpass filter (Figure 1e). The 1-min RMS averaged power in this band (Figure 1g) shows the well-known pulses of Pi2 power at substorm onset, the effect being greatest in the H component. Comparing with the measurements at Halley (Figures 1f and 1h), the power was lower at Faraday than Halley, and in fact in this case was only just above the instrument sensitivity (± 0.5 nT). Having looked at a single event, we will now use a super-posed epoch method, almost identical to that of our previous study [*Smith et al.*, 1999], to investigate the typical size and

relative timing of the different substorm signatures as a function of latitude and magnetic local time.

3.2. Superposed Epoch Analysis for a Near-Auroral Station $L \sim 4$ (Halley)

[9] As in our previous study, we used a number of criteria to select a set of epochs of the substorm expansion phase onset from our database of SCEs. The study was over the 4-year interval $1993-1996$, for which there were a total of 1043 events in the database. First, we required the epoch to be in the interval $0200-0400$ UT, i.e., within ~ 1 hour of
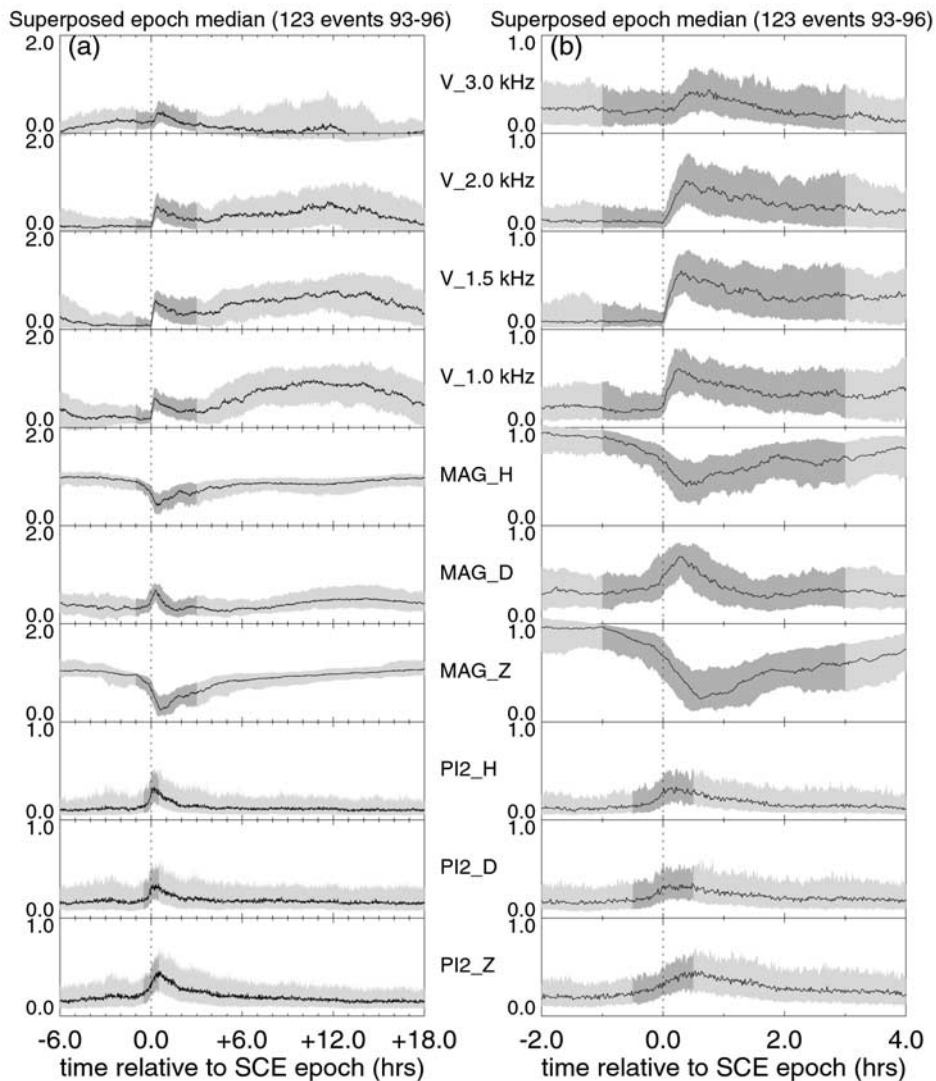
Figure 2. Medians and interquartile ranges of normalized epoch-aligned Halley data, obtained using 123 SCE epochs selected as described in the text. The epochs were from the years 1993–1996 and in the UT range 0200–0400 UT (2300–0100 MLT). From top to bottom are ELF/VLF wave intensities for four VELOX channels (3.0, 2.0, 1.5, 1.0 kHz), three magnetic components (H, D, Z) and three Pi2 power components (H, D, Z). (a) The time range from 6 hours before to 18 hours after the epoch, and (b) the range from -2 hours to $+4$ hours. The normalization interval around $t = 0$ is shown in a different shade from the rest of the interval.

local magnetic midnight (∼0300 UT). Second, if there was more than one event having its epoch within that time interval, we chose only the first. An additional criterion for the present study was that we required there to be no data gaps in the magnetic data, which would have caused problems in the filtering process. Applying the above criteria to the database yielded 123 events. All the data sets (ELF/VLF, magnetic bay and Pi2 power) were converted to 1-min time resolution as described above and normalized as described by *Smith et al.* [1999] so as to linearly transform the data points in the "normalization interval" to the range 0–1. This was done in order that a few large events did not distort the results. For the ELF/VLF and magnetic bay data the normalization interval was between -1 hour and $+3$ hours relative to the SCE epoch; for the Pi2 data, because of

its more transient character, the normalization interval was taken to be from -30 min to $+30$ min because it was expected to be more localized to the substorm onset. The data were then epoch-aligned and the median and quartile points found for each minute relative to the epoch, from 6 hours before to 18 hours afterward.

[10] Figure 2a shows the results of this process for four normalized VELOX channels (1.0, 1.5, 2.0, 3.0 kHz); the three normalized magnetic bay components H, D, and Z; and the corresponding three normalized Pi2 power components. In each panel the band represents the interquartile range, and the line represents the median. The normalization interval is shown by the darker grey. Figure 2b is an expansion of the range -2.0 hours to $+4.0$ hours. Changes are seen in the plotted parameters near the time of the SCE
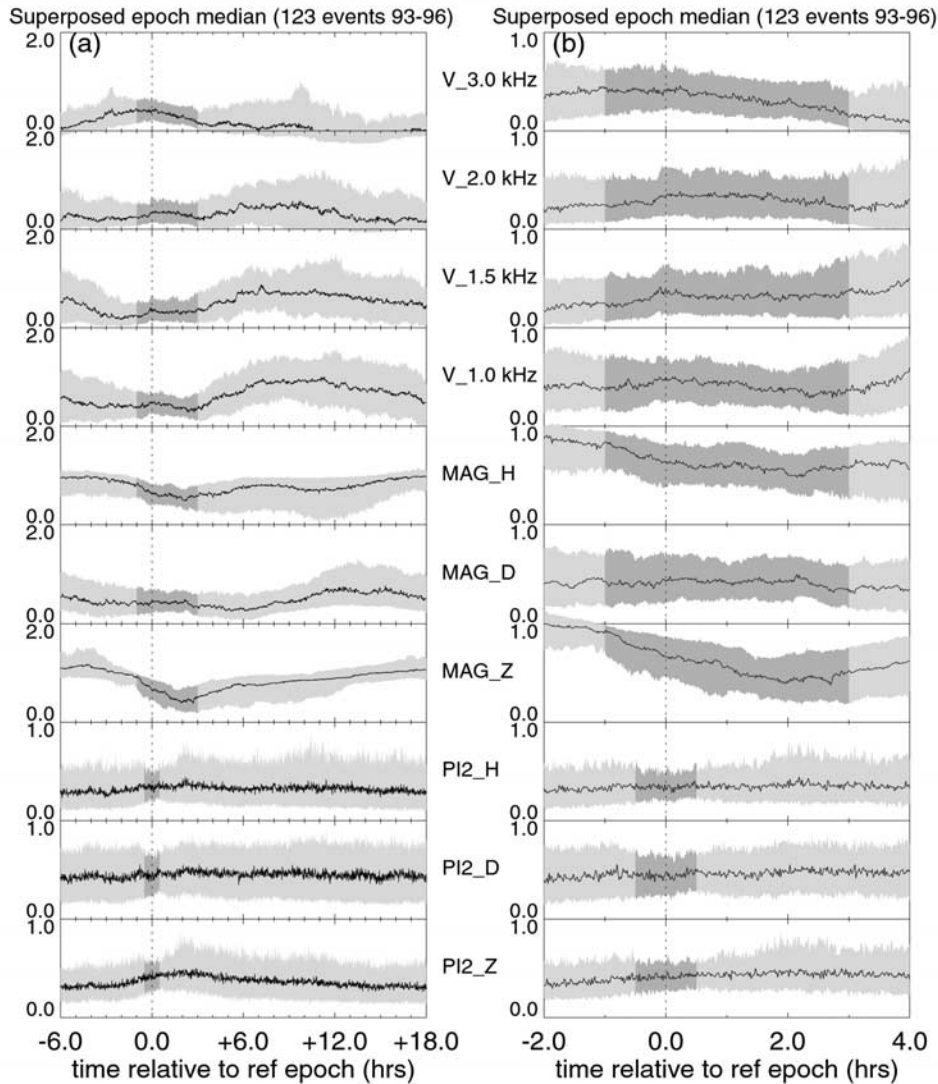
Figure 3. Similar to Figure 2 but for a nonsubstorm-related reference set of epochs, 24.0 hours earlier than the set of SCE epochs used in Figure 2.

($t = 0.0$ hours, shown by the vertical dashed line), but in order to distinguish the specific substorm response from any average background variation, we repeated the analysis for a set of 123 reference epochs not related to substorms. We required that these be "random" but with a similar distribution in local time, season, etc. to the set of SCE epochs; for this purpose we used the same set of epochs but shifted 24 hours earlier. The result is shown in Figure 3. As expected, there is a diurnal variation, but no effect is seen at $t = 0$.

[11] In the final stage of the data analysis the median curves of Figures 2 and 3 were "unnormalized," as described by *Smith et al.* [1999], using the reciprocal of the median of the scaling factors employed in performing the normalization. This was done in order to restore the original units and provide a quantitative measure of the substorm effect. The results are shown in Figures 4a–4c for the magnetic bay data and Figures 4d–4f for the Pi2 filtered data and are summarized in the first row of Table 1. Each panel contains one curve derived from the SCE set of epochs and one from the reference set. The difference between the two approximates to the substorm effect, which will be mainly from the DP1 (SCW) current system which switches on at the substorm expansion phase onset but may also include any substorm-related changes in DP2. The reference curve will have contributions from the DP2 and Sq current systems (plus a "smeared out" DP1 contribution around the zero epoch from any substorms that might have occurred on the reference day). To quantify the Sq contribution we also plot in Figures 4a–4c quiet day curves obtained from the zero-meaned daily magnetic variations at Halley for the quietest day of each month (the international q1 day, *Mayaud* [1980]) from March 1994 to December 1996, as provided by WDC-C2. The medians for these 21 days were detrended and shifted in time so that the 3 UT points (the center of the 0200–0400 UT time interval containing the SCE epochs) were aligned with the origin of epoch time. The difference between the reference and Sq curves approximately represents the DP2 effect (except possibly close to $t = 0$ where there may be the smeared
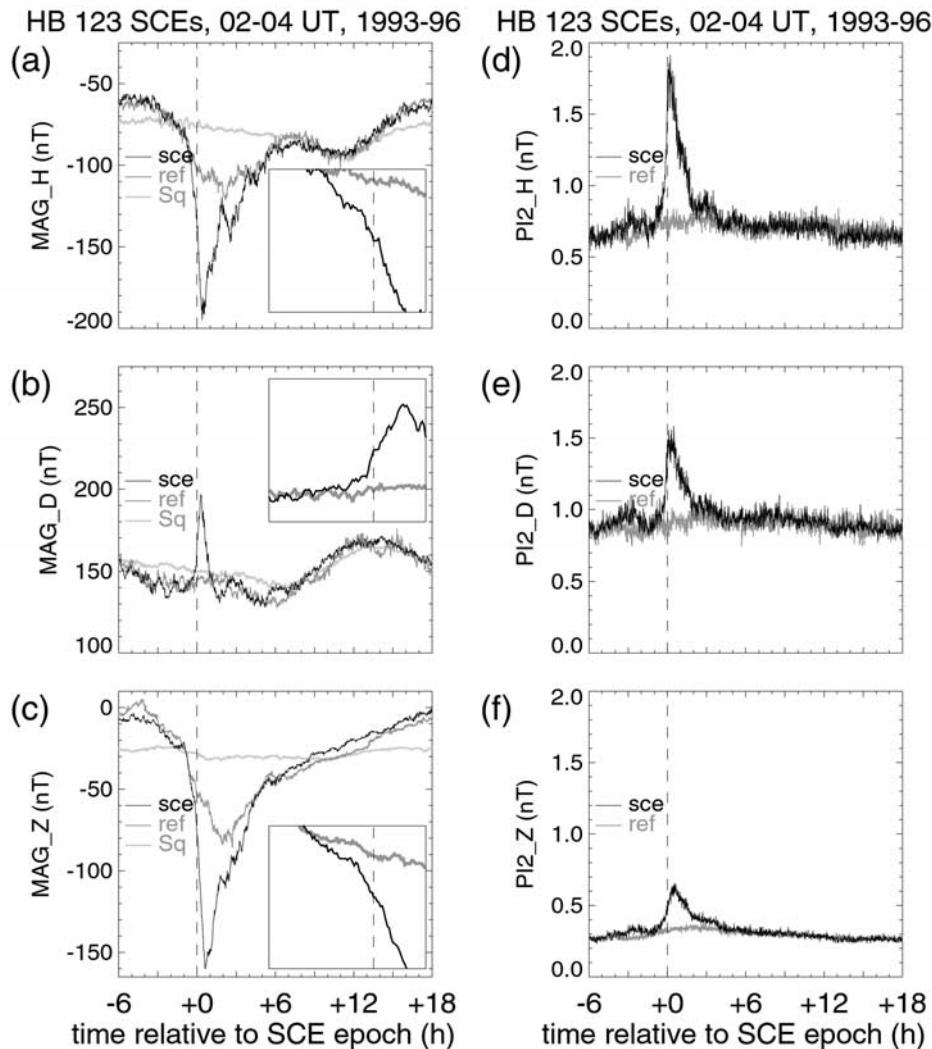
Figure 4. The results of "unnormalizing" the median curves of Figures 2 and 3 (see text for details), labeled "sce" and "ref," respectively. (a)–(c) The magnetic bay data taken from Figures 2a and 3a. The vertical scales of the panels are the same; the differing absolute values depend on instrument baselines and have no significance in the present context. The "sce" curve has been shifted vertically to match the "ref" curve well away from the substorm epoch (specifically so that their difference averaged over −6 hours to −5 hours and +17 hours to +18 hours is zero). The quiet day curves labeled "Sq" were derived as explained in section 3.2 and offset so as to coincide on average with the reference curves over the epoch time intervals 9–12 hours (for H and Z) and 15–18 hours (for D). These intervals correspond to 0600–0900 MLT and 1200–1500 MLT, local times when the contributions of the S_q current system to the reference curves are expected to be greatest relative to those of the DP2 system [*Chapman and Bartels*, 1940]. Small inset panels show the interval -60 min $\leq t < +30$ min with an expanded timescale; the vertical scale is the same as that of the main plot. (d)–(f) The median Pi2 power data taken from Figures 2a and 3a.

DP1 contribution). In Figures 4a–4c, the insets show the interval -60 min $\leq t < +30$ min in greater detail.

3.3. Superposed Epoch Analysis for a Midlatitude Station, $L \sim 2.5$ (Faraday)

[12] We repeated the analysis described above for Halley but using magnetometer data from Faraday in three different local time ranges. The substorm epochs were however still taken from the database of SCEs observed at Halley (there

is no VELOX instrument at Faraday). The first time range analyzed was 0200–0400 UT, i.e., the same as for the Halley study, when Faraday was in the premidnight local time sector, at approximately 2130–2330 MLT. We used a set of 282 SCE epochs taken from our database, distributed through the years 1992–1996. The results are shown in Figure 5, displayed in the same format as Figure 4, and summarized in Table 1. In a similar way to that described above for Halley, quiet day curves have been added which

Table 1. Magnetic Bay and Pi2 Amplitudes[a]

|			Bay (nT)			Pi2 (nT)		
			H	D	Z	H	D	Z
Halley	0200–0400 UT	(2300–0100 MLT)	−85	+50	−100	1.20	0.60	0.30
Faraday	0200–0400 UT	(2130–2330 MLT)	+8	−12	−7	0.15	0.10	0.10
Faraday	0300–0500 UT	(2230–0030 MLT)	+6	−7	−7	0.09	0.08	0.05
Faraday	0500–0700 UT	(0030–0230 MLT)	+2	−5	−8	0.09	0.05	0.06

[a]These are defined as the difference between the "sce" and "ref" curves, when the former is at its peak deviation. An exception is for the H bay component at Faraday, for which inspection of the plots suggests that noise on the "ref" curve would give a misleading result, and in this case we have used the peak deviation of the "sce" curve relative to its level just before $t = 0$.

have been derived from the zero-meaned daily magnetic variation at Faraday for the quietest day of each month in 1994–1996 (except November 1995, for which Faraday magnetic data were not available on the quietest day). In Figure 6 we present the results of a similar analysis using 189 SCE epochs in the range 0300–0500 UT, when Faraday was near local magnetic midnight (~2230–0030 MLT). Finally, Figure 7 shows the results for a set of 136 SCE
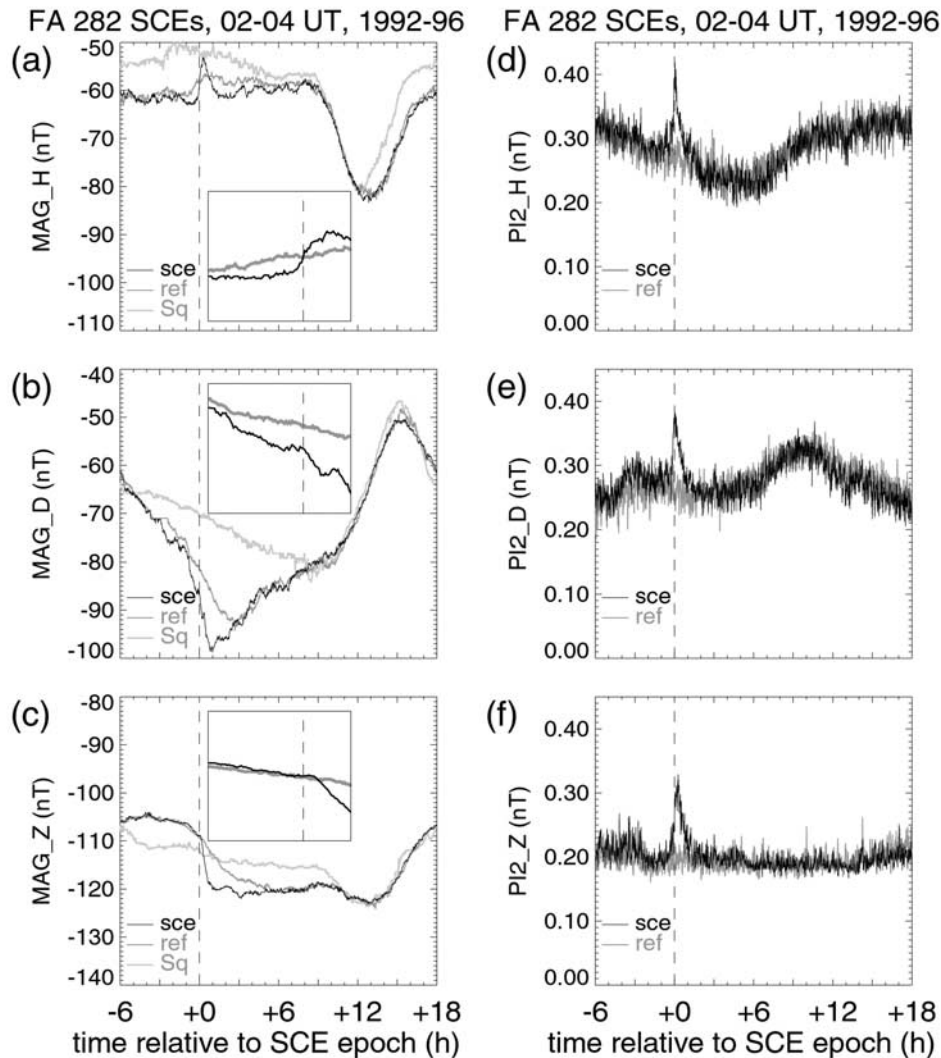
Figure 5. Similar to Figure 4 but for Faraday magnetic and Pi2 power data and a set of 282 SCE epochs in the range 0200–0400 UT (2130–2330 MLT). The vertical scales for the three components are the same as each other but different from those in Figure 4. The offsets for the "Sq" curves were based on local time ranges 0900–1100 MLT (for H and Z) and 0700–0900 MLT (for D).
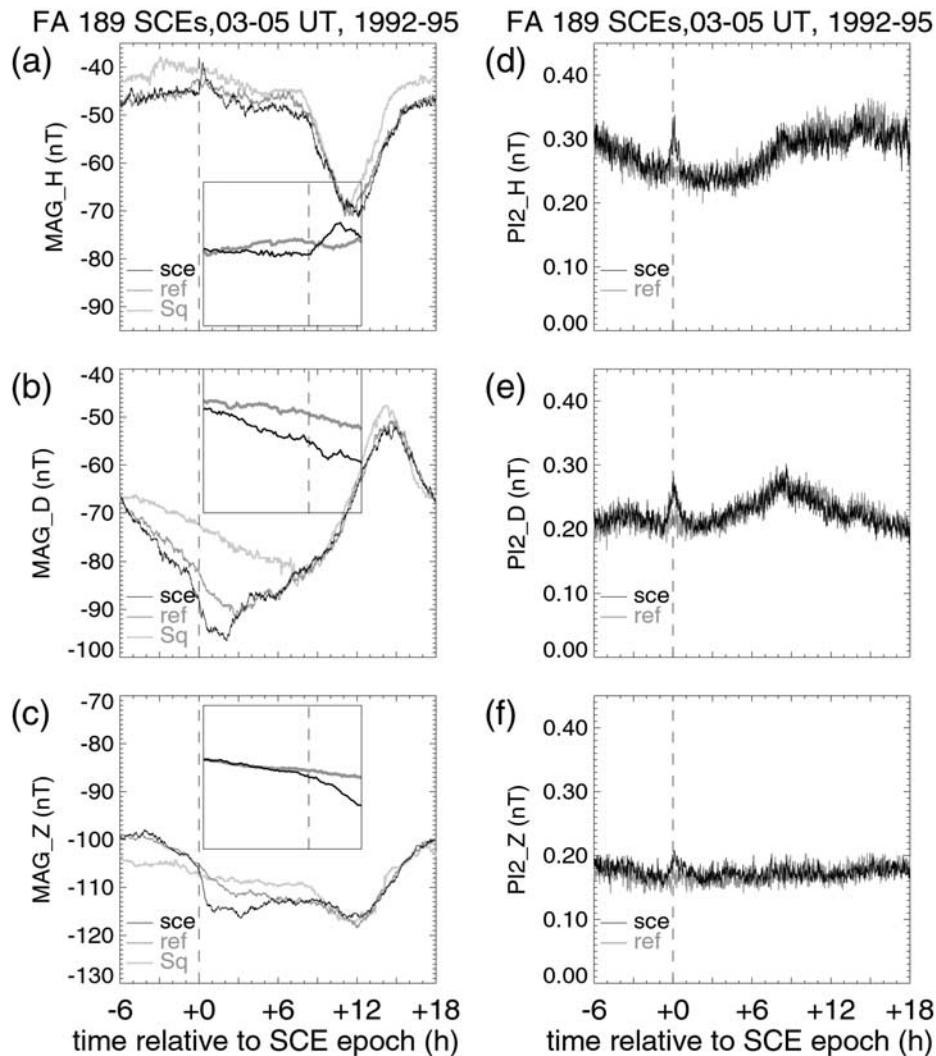
Figure 6. Similar to Figure 5 but for a set of 189 SCE epochs in the range 0300–0500 UT (2230–0030 MLT). The vertical scales are the same as in Figure 5.

epochs in the range 0500–0700 UT when Faraday was in the postmidnight sector (∼0030–0230 MLT).

4.   Discussion

4.1.   ELF/VLF Substorm Signature

[13] The upper four panels in Figure 2 represent the statistical shape of the ELF/VLF (chorus) response to a substorm, as observed at Halley when the station is close to magnetic midnight. The pronounced rise close to the SCE epoch is of course a consequence of using the SCEs observed in the ELF/VLF data to define the epochs for the superposed epoch analysis. We note in passing that this is a unique feature of the present work; previous studies of the statistical magnetic signature of a substorm have used different onset definitions; for example *Caan et al.* [1978] used the magnetic data themselves. We will not discuss the ELF/VLF results further, other than to note that the effect in the 3.0 kHz channel is delayed ∼10 min relative to that in the 1.5 kHz channel used to identify the epoch and that this provides an estimate of ∼0.15 kHz/min for the typical

frequency dispersion *df/dt* of the leading edge of an SCE. Thus by extrapolation the actual substorm onset may be estimated to occur up to ∼10 min prior to the epoch time, and this is probably a reasonable estimate of the uncertainty in the time of the substorm expansion phase onset when estimated from the SCE [*Smith et al.*, 1999].

4.2.   Magnetic Bay Signature

4.2.1.   Model

[14] We will discuss the magnetic bay response at both Halley and Faraday in terms of the well-known three-dimensional substorm current wedge (SCW) model in which downward and upward field-aligned currents, linking to the tail of the magnetosphere, close in the ionosphere forming the westward electrojet current [e.g., *McPherron et al.*, 1973].

[15] The magnetic field perturbations observed on the ground (δH, δD, δZ) from a SCW were worked out by *Kisabeth and Rostoker* [1977]. Here we use a formulation of the model which has been implemented at the University of York as part of a modeling package to derive SCW location
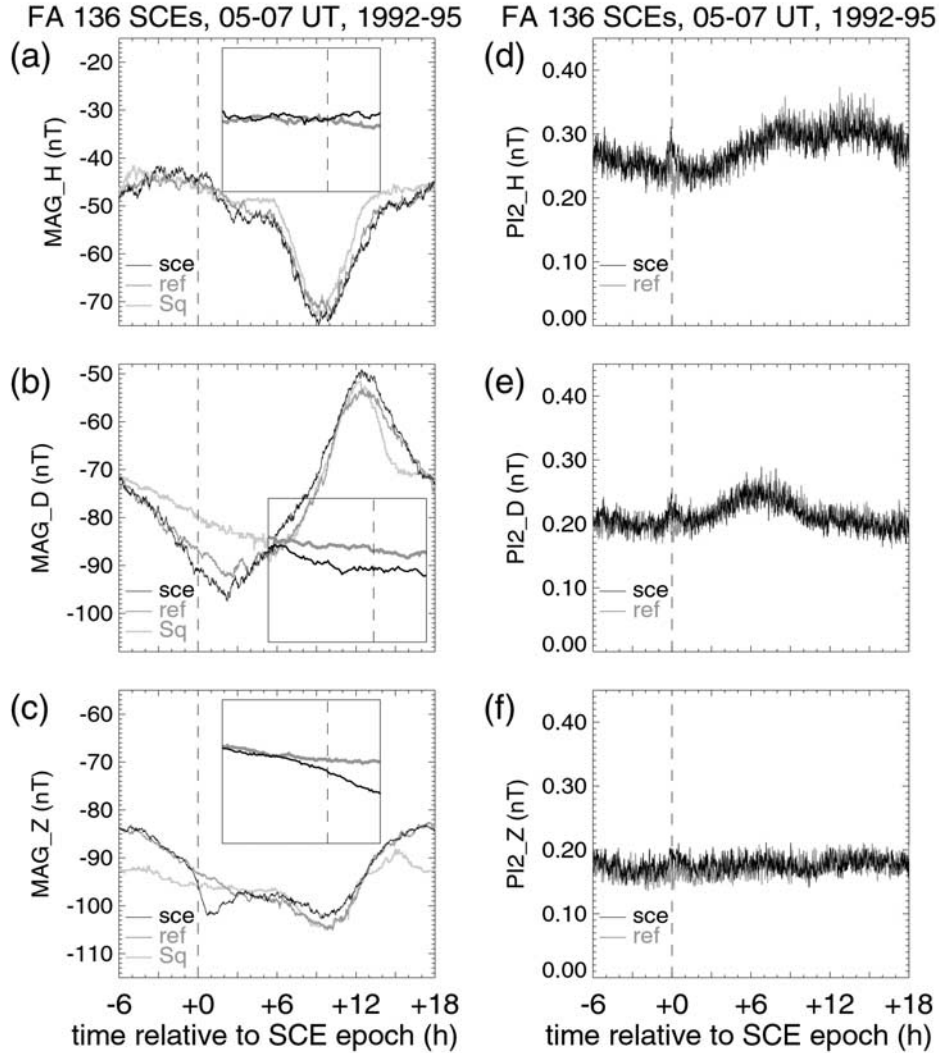
Figure 7. Similar to Figure 5 but for a set of 136 SCE epochs in the range 0500–0700 UT (0030–0230 MLT). The vertical scales are the same as in Figure 5.

and current growth from midlatitude magnetometer data [*Cramoysan et al.*, 1995]. The SCW is modeled as a pair of field-aligned currents flowing along dipole field lines, connected in the ionosphere by a westward electrojet and in the tail with the equatorial ring current. The field perturbations are computed at the surface of the earth which is represented as a sphere with a two-layer (i.e., one-dimensional) conductivity structure comprising a surface resistive layer overlying a superconducting core. Both the ionospheric and ground conductivities are assumed to be laterally isotropic. Maps of the ground magnetic field variations were presented by *Cramoysan et al.* [1995] (δH and δD) and *Bunting* [1995] (δZ). The δZ variation at midlatitude, which we discuss below, has been little considered in the literature. This is probably because the vertical variations can be suppressed by ground-induced currents in a homogeneous conductivity region or enhanced by local and regional conductivity structures.

[16] In the top row of panels in Figure 8 we present maps in MLT versus magnetic latitude coordinates of the modeled δH, δD, δZ in the Northern Hemisphere due to a current wedge 3 hours wide in MLT [*O'Pray*, 1998] with an electrojet at $67°$ latitude (the most probable latitude according to *Liou et al.* [2001]). The field perturbations for a 1 MA current and static geometry are shown in nT by the quasi-logarithmic scale. The next row is the corresponding set of plots for the Southern Hemisphere. In the bottom two rows the contributions of the electrojet and field-aligned currents to the Southern Hemisphere perturbations are shown separately. It is clear (as would be expected) that at points far from the electrojet, in either latitude or local time, its contribution is generally smaller than that of the field-aligned currents. Figure 8 is for just one choice of SCW parameters, whereas our data plots represent sets of substorms for which the electrojet latitude and MLT of the central meridian will vary from event to event.

4.2.2. Auroral Zone Signature at Halley

[17] We have derived the statistical shape and median amplitude, in H, D, Z, of the substorm magnetic bay at Halley (Figures 4a–4c and Table 1), namely a negative H,
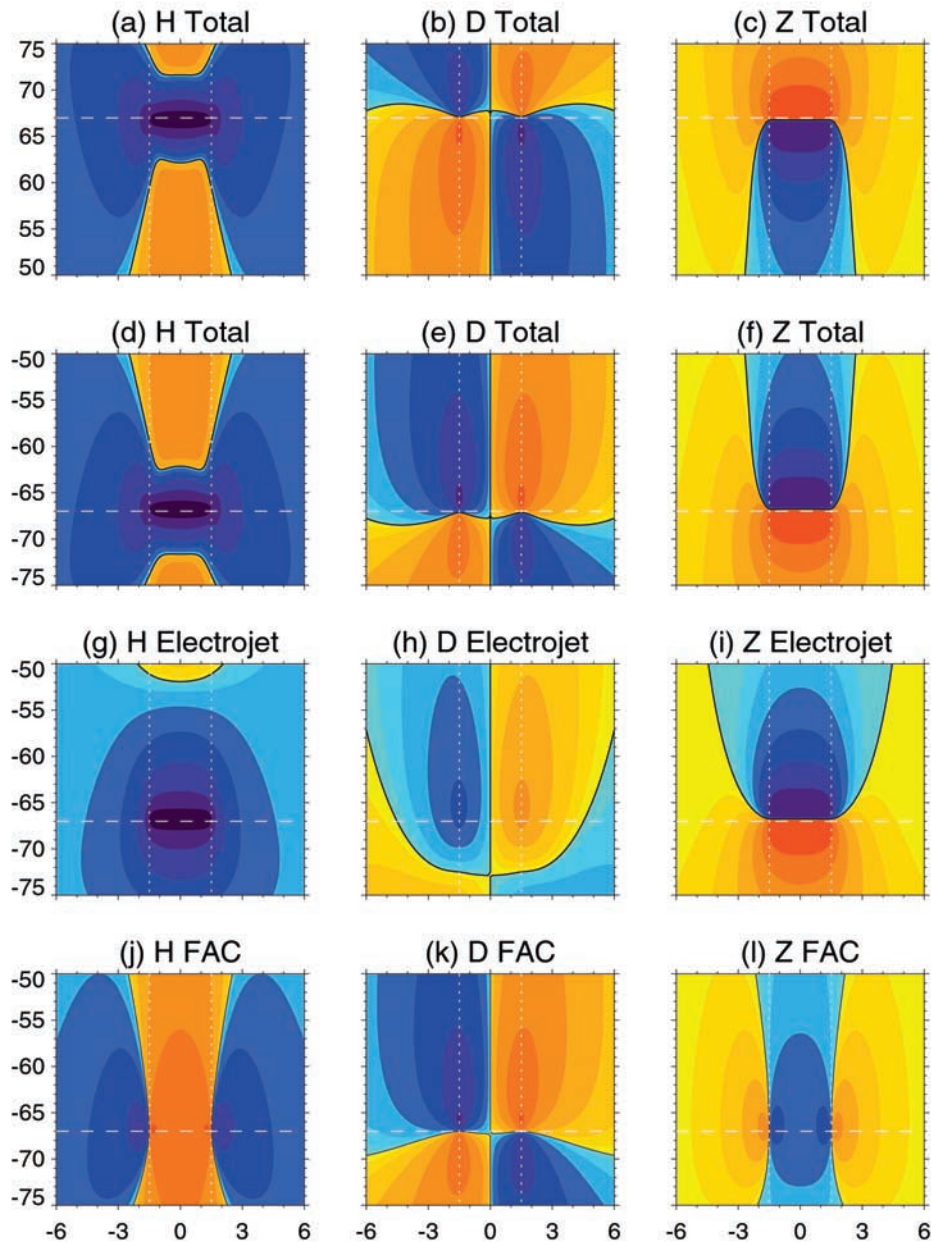
Figure 8. (a–c) Maps of δH, δD and δZ (north, east, and down components of magnetic perturbation) for the University of York SCW model (see text for details). Positive values, represented by yellows and reds of the quasi-logarithmic color scale, are separated by a solid black curve from negative values, represented by blues and purples. The horizontal dashed line marks the latitude of the westward electrojet (67°) and the vertical dotted lines indicate the meridians of the field-aligned currents, at ±1.5 hours MLT relative to the central meridian of the SCW. (d–f) Corresponding plots for the Southern Hemisphere. Here δH, δD and δZ are the north, east, and up components, the same sign convention as used for our data. The ratio of the δH and δZ medians at Halley are consistent with a station ~1.5 degrees equatorward of the electrojet, i.e., latitude 65.5° for the electrojet shown here (Halley's actual magnetic latitude is ~62°). The behavior at Faraday (~50°) is represented by the lower latitude boundary of the plots. (g–i) The separate contribution of the ionospheric (electrojet) part of the SCW to the Southern Hemisphere perturbations. (j–l) The separate contribution of the field-aligned current parts.

positive D, negative Z bay (δH ≃ −85 nT; δD ≃ +50 nT; δZ ≃ −100 nT). This is very similar to that published by *Smith et al.* [1999] (their Figure 6) who used a different but overlapping set of 258 SCE epochs between 1992 and 1995. The similarity is expected statistically but does confirm that the results are repeatable. The negative δH and δZ perturbations indicate a westward equivalent ionospheric current (electrojet), lying slightly to the south
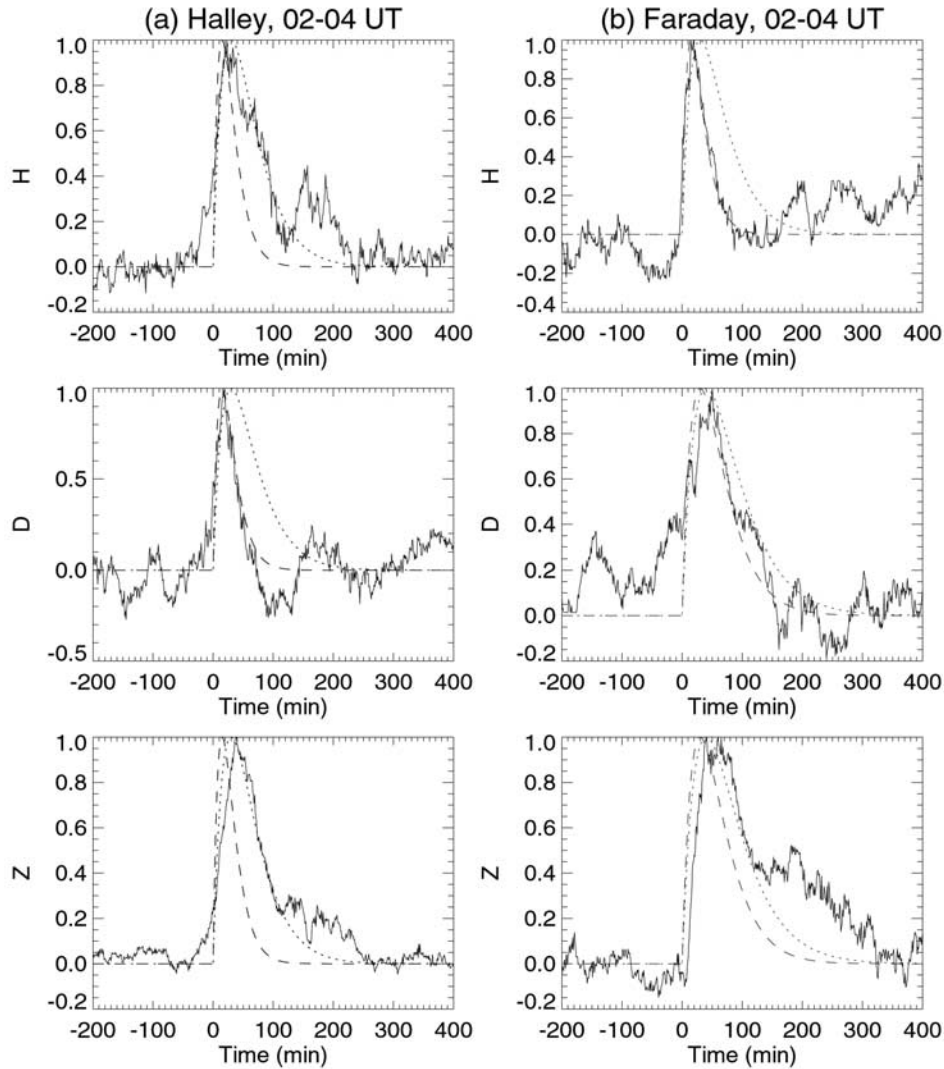
Figure 9. (a) The solid curves are "sce"-"ref" differences taken from the Halley data of Figures 4a–4c, normalized to 1 at the greatest absolute value of the difference (which occurs at $t \sim 20-50$ min). The dotted and dashed curves are the Weimer pulse waveforms $at \exp(-pt)$ for $p = 2$ h^{-1} and $p = 4$ h^{-1}, respectively, normalized by choosing $a = ep$. (b) Same as Figure 9a but for the Faraday premidnight case (Figures 5a–5c) except that for the H component only, for which inspection of the plots suggests that noise on the "ref" curve would give a misleading result, we have normalized the "sce" curve relative to its level at $t = -5$ min. The dotted and dashed curves are the normalized Weimer pulse waveforms for $p = 2$ h^{-1} and $p = 4$ h^{-1}, respectively (H) and $p = 1.5$ h^{-1} and $p = 2$ h^{-1}, respectively (D and Z).

(poleward) of Halley; this is in qualitative agreement with the model of Figures 8d–8f. The positive δD may be the result of a tendency of the center of the current wedge to be earlier in local time than the observing station, i.e., premidnight in this case; though *Smith et al.* [1999] attributed it to a local effect at Halley in which the electrojet current had a slight geomagnetically southward component [*Boteler*, 1978]. The substorm effect is smaller than in the example of Figure 1d because it includes the effects of many events, most of which may be smaller (owing to a weaker or more distant electrojet current) than the example. Of interest is the secondary peak at $t \simeq 2.5$ hours, evidence of the tendency of substorms to recur on this timescale [e.g., *Borovsky et al.*, 1993]; this is also seen clearly in Figure 9, described below.

[18] The reference and sce curves diverge ~ 30 min prior to $t = 0$; this is more than the ~ 10 min uncertainty in the onset time and is interpreted as an enhancement in the DP2 current system prior to the substorm expansion phase onset. There is a short levelling of the curves (inflection), in H and Z and possibly also D, just before onset. This feature was found and noted in the AL index by *Caan et al.* [1978] but not explained. It could be due to the auroral fading phenomenon [*Kauristie et al.*, 1997] or the effect on DP2 of reduced convection associated with a northward turning of the interplanetary magnetic field which could occur prior to the triggering of a substorm [*Lyons et al.*, 2001].

[19] As implied above, it is difficult to be sure how much of the difference between the "sce" and "ref" curves is

due to DP1, though any changes at $t = 0$ such as the gradient enhancement in H and Z will be. In order to focus on the time dependence of the substorm effect, we plot in Figure 9 the normalized difference between the "sce" and "ref" variations. In Figure 9a, for example, the Halley H, D and Z "sce"-"ref" differences (solid curves) are normalized to 1 at their greatest absolute values (which occur at $t \sim 20$–30 min). An interesting feature is the faster recovery to the presubstorm levels in the D component compared with H and Z. This may be analyzed in terms of the "Weimer pulse" waveform [*Weimer*, 1994]: at $\exp(-pt)$, normalized Weimer pulses for $p = 2$ h^{-1} and $p = 4$ h^{-1} are shown as dotted and dashed curves in the figure. It appears that $p = 2$ h^{-1} is a good fit to the H and Z data, while $p = 4$ h^{-1} fits the D variation better. In his superposed epoch analysis of the AL index substorm bay, *Weimer* [1994] also found $p = 2$ h^{-1} to give the best fit. The waveform was the solution to a second-order differential equation describing the impulsive response of the current (and hence ground magnetic perturbation) in an electrical circuit similar to the SCW, in which $p = -1/2RC$ where C is the capacitance of the SCW and R is the ionospheric resistance. If the geometry of the SCW and its position relative to the observing station remained constant during the substorm, a decaying current in the wedge would be expected to affect all components with the same time constant. The fact that this is not observed may be because the geometry is changing.

[20] A possible explanation can be proposed in the context of Figure 8. The initial perturbation in D at Halley is positive, which indicates that it was initially equatorward of the electrojet and eastward of its center. If the station was just equatorward of the electrojet and the current wedge was widening during the recovery phase, the station would effectively be moving closer to the center of the wedge, toward a smaller D perturbation (contours run approximately north–south), thus giving a faster relaxation rate for the D component as observed. In contrast, the effect of the relative motion would be small on H and Z (contours run approximately east–west).

4.2.3. Midlatitude Signature at Faraday

[21] In a similar fashion to that described above for Halley we have derived the statistical shape and median amplitude, in H, D, Z, of the substorm magnetic bay at Faraday but now for three different local magnetic time ranges: premidnight, midnight, and postmidnight (Figures 5a–5c, 6a–6c, and 7a–7c, respectively, and Table 1). The three cases are more closely spaced than those considered by *Caan et al.* [1978] who presented results for dawn, noon, dusk, and midnight.

[22] The premidnight substorm magnetic bay response, shown in Figures 5a–5c, is naturally much smaller than at the near-auroral station and is positive in H and negative in D ($\delta H \simeq +8$ nT; $\delta D \simeq -12$ nT). This is the expected behavior for a midlatitude ground station on the westward side of the center of the substorm current wedge [*Rostoker et al.*, 1980] and is consistent with Figure 8. H begins to change close to onset as expected, but D appears to diverge from the reference curve ~ 1 hour earlier, most likely owing to enhancement of the DP2 current system during the substorm growth phase. Note that this midlatitude DP2 signature is opposite to what one might expect at auroral

latitudes for equatorward flow out of polar cap [*Chapman and Bartels*, 1940].

[23] There is then a gradient change in D at $t = 0$, immediately preceded by an "inflection point" similar to that seen in the Halley H and Z components (see above). Since Faraday is distant from the auroral zone, this may favor the explanation in terms of the IMF northward turning. This is because a northward turning of the IMF would be expected to reduce the DP2 current globally, whereas auroral fading would reduce the DP2 current only locally in the auroral zone.

[24] The clear long-lived (~ 5 hours) negative Z bay ($\delta Z \simeq -7$ nT) begins at onset. *Rostoker* [1972] suggested that the Z-component bay at midlatitudes is mostly due to the westward electrojet, but Figures 8i and 8l imply that the contribution from the field-aligned segments of the current wedge is as great, though both produce a negative Z perturbation (upward in the Northern Hemisphere and downward in the Southern Hemisphere). The model correctly predicts that the midlatitude $|\delta H|$ and $|\delta Z|$ are of comparable magnitude. For example at $-50°$ latitude near the western FAC meridian, Figures 8d and 8f show both to be ~ 10 nT.

[25] In Figure 9b we compare the observed normalized bay data with a normalized Weimer pulse as we did for Halley. In this case the D component curve fits the waveform well with $p = 2$ h^{-1}. As for H and Z in the near-auroral zone case, this may represent the effect of the current decay alone, since in Figure 8a the D contours are roughly east–west at low latitudes near the meridian of the westward field-aligned current. In contrast, the H and Z contours are more nearly north–south, and a geometrical contribution from a changing configuration due to eastward motion of the observing station in local time, and/or expansion of the wedge, would be expected. This would lead to a slower recovery, as observed for Z ($p = 1.5$ h^{-1}) but not H ($p = 4$ h^{-1}).

[26] The near-midnight study (Figure 6) shows similar features to the premidnight case, with positive H and negative Z bays ($\delta H \simeq +6$ nT; $\delta Z \simeq -7$ nT) beginning at onset, and a negative D bay ($\delta D \simeq -7$ nT) beginning earlier and showing only a slight gradient change at $t = 0$. The similarity is perhaps not surprising, given the 50% overlap in the UT intervals in the two cases, and a difference of only 1 hour in MLT. The H and Z bays are similar in size to the premidnight case, consistent with the model of Figure 8 which shows that δH and δZ vary little within the current wedge at midlatitudes. On the other hand the size of the D bay is about half that of the premidnight δD, consistent with a change to an observation point nearer to, but slightly west of, the central meridian. As in the premidnight case, part of the bay may be due to an enhanced DP2 current rather than entirely DP1. A comparison with the normalized Weimer function (not shown) is less clear than for premidnight because of the poorer signal-noise ratio of the bay; however it does not appear to show any significantly different behavior from Figure 9b.

[27] In the post-midnight case (Figure 7) the trends from premidnight to near midnight are continued. The H bay has become even smaller and is barely seen above the noise ($\delta H \lesssim +2$ nT). This may indicate that the observing station is located outside the substorm current wedge, near the

eastern edge of the low-latitude positive H region (Figure 8); however this would not explain why the Z bay continues to be observed and is in fact now the dominant component ($\delta Z \simeq -8$ nT). There is now little evidence of a DP1 contribution to δD (no gradient change at $t = 0$ and no minimum at $t \sim +30$ min), whereas the model would predict an increase in $|\delta D|$ from the center to the edge of the SCW.

4.3. Pi2 Signature
4.3.1. Halley

[28] We have derived the statistical shape and median RMS amplitude of the power in the 40–150 s (7–25 mHz) Pi2 band at Halley (Figures 4d–4f and Table 1). Referred to the reference curves, this is largest in the H component and begins about an hour before the SCE onset, peaking almost exactly at onset in H and D with an RMS amplitude of $\delta H \simeq$ 1.2 nT and $\delta D \simeq 0.6$ nT. The Z component is the smallest ($\delta Z \simeq 0.3$ nT) and peaks ~30 min later.

[29] Comparing Figures 4a–4c with Figures 4d–4f, we see that in contrast to the lower latitude Pi2 response discussed below, there is a close correspondence/proportionality between the magnetic H, D, Z perturbations from the reference curves (which have effectively been bandpass-filtered between 1 day^{-1} and 1 min^{-1}) and the corresponding wave power in the Pi2 frequency band. Furthermore, the Pi2 wave power increases prior to the SCE epoch. These observations indicate that wave power in the Pi2 frequency band at this near-auroral location of Halley is primarily part of a broader band wave spectrum in which the power in the lower frequencies is related to the power in the Pi2 frequency band. This is consistent with the perturbations arising from the power law spectrum of a turbulent scale-free DP2 electrojet current [e.g., *Weimer et al.*, 1985].

[30] The close relationship between the low-frequency and Pi2 band behavior is broken slightly near substorm onset where the Pi2 amplitude in the H and D components peaks immediately after the SCE epoch whereas the low-frequency bay signature peaks slightly later at $t = 20$–30 min, the end of the substorm expansion phase. Thus there appears to be a secondary, narrow-band Pi2 component that is likely associated with the formation of the DP1 electrojet current during the substorm expansion phase.

4.3.2. Faraday

[31] In a similar fashion to that described above for Halley we have derived the statistical shape and median RMS amplitude of the power in the 40–150 s (7–25 mHz) Pi2 band at Faraday for the three different local magnetic time ranges (Figures 5d–5f, 6d–6f, and 7d–7f, respectively, and Table 1).

[32] For the premidnight case (Figures 5d–5f), the 40–150 s intensity results show the classic midlatitude Pi2 response [*Saito et al.*, 1976], peaking at RMS amplitudes of ~0.1 nT in all three components (about a tenth of the size of the corresponding peak at Halley). In contrast to Halley, there is no increase before onset, and the peak has a duration (<1 hour) that is shorter than the bay, consistent with a dominant contribution from a substorm associated Pi2 pulsation burst occurring at the expansion phase onset.

[33] Near midnight (Figures 6d–6f) the 40–150 s Pi2 intensity is somewhat smaller (see Table 1), and for the post-midnight case (Figure 7d–7f) it is smaller still. The

progressively decreasing Pi2 powers seen with increasing MLT suggest a center of activity biased to the evening side of midnight (see *Sutcliffe* [1980] who found that Pi2s at Hermanus were most likely to be seen when the SCW was centered 40° to the east of the station); alternatively, the result may imply preferred propagation of the Pi2 pulsations toward the evening local time sector.

5. Summary and Conclusions

[34] In this paper we have extended the work of *Smith et al.* [1999] to determine the "typical" (or median) magnetic bay and Pi2 substorm responses at near-auroral and mid-latitude ground stations (Halley and Faraday stations, respectively) over a large number (100–300) of substorms. The method is based upon a superposed epoch analysis, with sets of epochs of substorm expansion phase onset taken from a database of substorm chorus events (SCEs) observed by the VELOX VLF/ELF receiver at Halley. The spatial and temporal properties of the magnetic bay substorm signature are compared against a University of York variant of the *Kisabeth and Rostoker* [1977] substorm current wedge model and the *Weimer* [1994] pulse model, respectively. This has produced the following results:

1. The observed spatial variation of the DP1 component of the median substorm magnetic bay signature can be explained by the York model for a SCW 3 hours wide in local time, centered slightly before midnight MLT, and westward electrojet at latitude 67°. This model thus remains a useful framework within which to interpret substorm signatures, even though a recent study by *Weimer* [2001] has shown that the actual distribution of field-aligned currents, and hence horizontal currents, is more complex.

2. The rarely discussed Z component of the substorm magnetic bay signature is shown to be well-defined and similar to that expected by the York SCW model. It is commonly the clearest and largest DP1 signature at Halley and Faraday.

3. The York SCW model does not predict the absence of a gradient change in D at onset or the dominance of the Z component in the postmidnight MLT sector. Presumably, a more sophisticated model is required to explain these postmidnight observations.

4. The temporal shape of the DP1 component of the magnetic bay substorm signature fits a normalized Weimer pulse well. The decay rate of the H and Z components at Halley and the D component at Faraday is $p = 2$ h^{-1} and matches that found by *Weimer* [1994] for the AL index. This is interpreted in terms of a decaying current in the wedge. However, the recovery time constants are different for δD at Halley ($p = 4$ h^{-1}) and for δH ($p = 4$ h^{-1}) and δZ ($p = 1.5$ h^{-1}) at Faraday. The former two are postulated to be due to an additional geometrical contribution, arising from a changing wedge configuration relative to the observing station (possibly widening during the recovery phase). The latter cannot be understood qualitatively in the same terms.

5. A secondary bay in the superposed epoch plots at about $t = 2.5$ hours confirms the tendency of substorms to repeat with this period.

6. The amplitude of the DP2 component of the magnetic bay substorm signature is comparable with that of the DP1 component. The DP2 component is predominantly in H and

Z at Halley at midnight MLT and in *D* at Faraday between 2230 and 0230 MLT. It is enhanced ∼40 min prior to substorm onset.

7. An inflection point in *H* and *Z* at Halley is seen just prior to onset. This could be related to auroral fading or reduced convection associated with northward turning of the IMF. The same inflection point is seen in *D* at Faraday, probably favoring the latter explanation.

8. The median substorm signature at Halley in the Pi2 frequency band (7−25 mHz) appears to be related to the bay structure, implying that it is part of a broad band turbulent spectrum in the substorm-dependent DP2 current, though there is evidence of an additional minor narrow band component occurring at substorm onset.

9. At Faraday we see the classic midlatitude substorm signature: a short Pi2 pulsation burst at onset. The observed Pi2 power decreases progressively with increasing local time, possibly implying a source region biased to the evening side or else preferred propagation to the west from a near-midnight source.

10. The typical frequency dispersion of the leading edge of an SCE is *df/dt* ∼0.15 kHz/min; the SCE-inferred substorm onset time can be estimated to an accuracy of ∼10 min or better.

References

Borovsky, J. E., R. J. Nemzek, and R. D. Belian, The occurrence rate of magnetospheric-substorm onsets: Random and periodic substorms, *J. Geophys. Res.*, *98*, 3807, 1993.

Boteler, D. H., The effect of induced currents in the sea on magnetic bays observed at a coastal observatory, *J. Atmos. Terr. Phys.*, *40*, 577−580, 1978.

Bunting, R. J., Development and use of a current wedge modelling method for analysis of multiple onset substorms, D. Phil. thesis, University of York, York, U.K., 1995.

Caan, M. N., R. L. McPherron, and C. T. Russell, The statistical magnetic signature of magnetospheric substorms, *Planet. Space Sci.*, *26*, 269, 1978.

Chapman, S. and J. Bartels, *Geomagnetism*, Oxford Univ. Press, New York, 1940.

Cotton, P. D., and D. A. Simmons, The geomagnetic observatory at Faraday, Argentine Islands, *Polar Rec.*, *23*, 192, 1986.

Cramoysan, M., R. Bunting, and D. Orr, The use of a model substorm wedge in the determination of the position of substorm current systems, *Ann. Geophys.*, *13*, 583, 1995.

Dudeney, J. R., A. S. Rodger, A. J. Smith, M. J. Jarvis, and K. Morrison, Satellite Experiments Simultaneous with Antarctic Measurements (SE-SAME), *Space Sci. Rev.*, *71*, 705, 1995.

Kamide, Y., and H. W. Kroehl, Auroral electrojet activity during isolated substorms at different local times—A statistical study, *Geophys. Res. Lett.*, *21*, 389, 1994.

Kauristie, K., T. I. Pulkkinen, A. Huuskonen, R. J. Pellinen, H. J. Opgenoorth, D. N. Baker, A. Korth, and M. Syrjasuo, Auroral precipitation fading before and at substorm onset: Ionospheric and geostationary signatures, *Ann. Geophys.*, *15*, 967, 1997.

Kisabeth, J. L., and G. Rostoker, Modelling of three-dimensional current systems associated with magnetospheric substorms, *Geophys. J. R. Astron. Soc.*, *49*, 655, 1977.

Liou, K., P. T. Newell, D. G. Sibeck, C. I. Meng, M. Brittnacher, and G. Parks, Observation of IMF and seasonal effects in the location of auroral substorm onset, *J. Geophys. Res.*, *106*, 5799, 2001.

Lyons, L. R., J. M. Ruohoniemi, and G. Lu, Substorm-associated changes in large-scale convection during the November 24, 1996, Geospace Environment Modeling event, *J. Geophys. Res.*, *106*, 397, 2001.

Mayaud, P. N., *Derivation, Meaning, and Use of Geomagnetic Indices*, AGU, Washington D. C., 1980.

McPherron, R. L., C. T. Russell, and M. P. Aubry, Satellite studies of magnetospheric substorms on August 15, 1968, 9, Phenomenological model for substorms, *J. Geophys. Res.*, *78*, 3131, 1973.

O'Pray, P. E., The modeling of substorm current wedge locations using different magnetometer networks, D. Phil. thesis, University of York, York, U.K., 1998.

Rostoker, G., Interpretation of magnetic field variations during substorms, in *Earth's Magnetospheric Processes*, edited by B. M. McCormac, pp. 379−390, D. Reidel, Norwell, Mass., 1972.

Rostoker, G., S.-I. Akasofu, J. Foster, R. A. Greenwald, Y. Kamide, A. T. Y. Lui, R. L. McPherron, and C. T. Russell, Magnetospheric substorms—Definitions and signatures, *J. Geophys. Res.*, *85*, 1663, 1980.

Saito, T., K. Yumoto, and Y. Koyama, Magnetic pulsation Pi2 as a sensitive indicator of magnetospheric substorm, *Planet. Space Sci.*, *24*, 1025, 1976.

Smith, A. J., VELOX: A new VLF/ELF receiver in Antarctica for the Global Geospace Science mission, *J. Atmos. Terr. Phys.*, *57*, 507, 1995.

Smith, A. J., M. P. Freeman, and G. D. Reeves, Postmidnight VLF chorus events, a substorm signature observed at the ground near *L* = 4, *J. Geophys. Res.*, *101*, 24,641, 1996.

Smith, A. J., Correction to "Postmidnight VLF chorus events, a substorm signature observed at the ground near *L* = 4", *J. Geophys. Res.*, *102*, 2433, 1997.

Smith, A. J., M. P. Freeman, M. G. Wickett, and B. D. Cox, On the relationship between the magnetic and VLF signatures of the substorm expansion phase, *J. Geophys. Res.*, *104*, 12,351, 1999.

Sutcliffe, P. R., The longitudinal range of Pi 2 propagation at low latitudes, *Planet. Space Sci.*, *28*, 9, 1980.

Weimer, D. R., Substorm time constants, *J. Geophys. Res.*, *99*, 11,005, 1994.

Weimer, D. R., Maps of ionospheric field-aligned currents as a function of the interplanetary magnetic field derived from Dynamics Explorer 2 data, *J. Geophys. Res.*, *106*, 12,889, 2001.

Weimer, D. R., C. K. Goertz, D. A. Gurnett, N. C. Maynard, and J. L. Burch, Auroral zone electric fields from DE 1 and 2 at magnetic conjunctions, *J. Geophys. Res.*, *90*, 7479, 1985.

————————

M. P. Freeman, A. J. Smith, and S. Hunter, British Antarctic Survey, High Cross, Madingley Road, Cambridge CB3 0ET, UK. (m.freeman@bas.ac.uk; a.j.smith@bas.ac.uk)

D. K. Milling, Department of Physics, University of York, York YO10 5DD, UK. (dave@samsun.york.ac.uk)